Using NGRDI index to assist in forest canopy gaps classification of UAV RGB imagery

Yu-Xuan Zhan[1], Yong-Jun Zhang[2], Chun-Hung Wei[3], Jan-Chang Chen[4]

[1] General Research Service Center / Doctoral Program in Bioresources, National Pingtung University of Science and Technology(NPUST), 1, Shuefu Road, Neipu, Pingtung 912301, Taiwan (R.O.C.)-yxzsunny@mail.npust.edu.tw

[2] Dept. of Forestry, National Pingtung University of Science and Technology(NPUST), 1, Shuefu Road, Neipu, Pingtung 912301, Taiwan (R.O.C.)-b0979026785@gmail.com

[3] Dept. of Forestry, National Pingtung University of Science and Technology(NPUST), 1, Shuefu Road, Neipu, Pingtung 912301, Taiwan (R.O.C.)-aw711212@gmail.com

[4] Dept. of Forestry, National Pingtung University of Science and Technology(NPUST), 1, Shuefu Road, Neipu, Pingtung 912301, Taiwan (R.O.C.)-janchang17@gmail.com

Keywords: Canopy gaps, UAV-RGB imagery, vegetation Indices, Normalized Green–Red Difference Index (NGRDI).

Abstract

The formation of canopy gaps alters forest microclimates, influencing understory regeneration, soil organic matter decomposition, and nutrient cycling, thereby playing a crucial role in forest ecology. Traditional methods for detecting canopy gaps typically rely on multispectral imagery or LiDAR data, which are accurate but costly and technically demanding. In recent years, several studies have explored the feasibility of using UAV-based RGB imagery for gap detection. This study utilized UAV RGB imagery to analyze the temporal dynamics of canopy gaps to assess the feasibility of employing RGB-based vegetation indices for canopy gap detection. The Normalized Green–Red Difference Index (NGRDI) combined with DSM differencing was used for analysis. Results show that when NGRDI < 0.03, forest areas can be effectively categorized into two classes: “canopy gaps” and “canopy cover.” The overall classification accuracy reached 93% with a Kappa coefficient of 0.68. However, the omission error was 44.44%, which suggests that the model requires improvement in detecting small or edge gaps. It is recommended that identified threshold be used as a preliminary criterion for “canopy versus non-canopy” classification, supplemented with DSM or CHM data to improve detection accuracy.

1. Introduction

Forest canopy gaps are openings in the canopy caused by tree falls, mortality, or breakage, which modify the understory light, temperature, and humidity, thus facilitating plant regeneration and growth (Brokaw, 1982). Gap formation can result from natural disturbances—such as windstorms, heavy rainfall, pests, and aging, or anthropogenic factors such as logging and forest management (Whitmore, 1989). Increasing gap area or frequency indicates canopy opening and decreased coverage, driven by aging, pest damage, extreme weather, or thinning operations (Muscolo et al., 2014; Mazdi et al., 2021; Winstanley et al., 2024). Conversely, when canopy closure occurs, gaps diminish as residual crowns expand laterally, saplings and understory vegetation grow vertically, or artificial regeneration accelerates canopy recovery (Muscolo et al., 2014; Krüger et al., 2023; Winstanley et al., 2024). Canopy gaps significantly influence microclimatic conditions which in turn affect understory diversity, ecological processes such as decomposition and nutrient cycling, and overall forest dynamics (Zhu et al., 2014; Lenk et al., 2024; Tian et al., 2024).

LiDAR-based canopy gap detection offers high structural accuracy but remains costly and computationally demanding compared with UAV-RGB systems (Gaulton & Malthus, 2008; Chung et al., 2022). Consequently, UAV RGB imagery has become an increasingly attractive alternative due to its lower cost, high spatial resolution, and operational flexibility. Recent applications demonstrate that UAV imagery can effectively detect small canopy openings and capture short-term structural changes, and it can be further integrated with deep learning models for automated monitoring (Chen et al., 2023; Simonetti et al., 2023; Htun et al., 2024). However, in heterogeneous forests with complex terrain, shadowing effects and illumination variability continue to undermine gap-classification accuracy, highlighting the need for contextual calibration or auxiliary structural data.

RGB imagery provides not only high-resolution two-dimensional spatial information but also enables vegetation assessment through visible-spectrum indices such as the Normalized Green–Red Difference Index (NGRDI), Excess Green Index (ExG), and Visible Atmospherically Resistant Index (VARI) (Biró et al., 2024). Among these indices, NGRDI—derived from normalized differences between red and green reflectance—has demonstrated strong resistance to illumination variability and is therefore particularly well suited for detecting vegetation cover changes and identifying structural disturbances across large areas. Its simplicity, computational efficiency, and stability under varying light conditions make NGRDI a practical choice for UAV-based ecological monitoring.

Accordingly, this study utilized UAV-derived RGB imagery to investigate the temporal dynamics of forest canopy gaps and to assess the feasibility of applying RGB-based vegetation indices for identifying the spatial distribution of canopy openings. Through this approach, the study aimed to determine whether visible-spectrum indices can reliably capture structural changes in forest canopies and support gap-detection analyses in environments where more advanced multispectral or LiDAR sensors may not be available.

2. Method

2.1 Study Area

The study was conducted in Siangjiao Bay Ecological Reserve, located within Kenting National Park in southern Taiwan, between 21°56´ – 21°57´ N and 120°49´ – 120°50´ E. The reserve covers 28.48 ha, bisected by Provincial Highway 26

https://doi.org/10.5194/isprs-archives-XLIX-B3-2026-325-2026

(Figure 1). The region features a typical coral reef coastal landscape with complex shorelines, intertidal zones, and sandy beaches. The tropical monsoon climate has an annual mean temperature of approximately 26°C and precipitation of 2,000–2,500 mm, concentrated during summer typhoons. Sea temperatures exceed above 25°C annually due to Kuroshio Branch, fostering diverse coastal ecosystems. Terrestrial vegetation includes tropical coastal shrubs and windbreak species such as *Barringtonia asiatica* (L.) Kurz., *Hernandia nymphiifolia* (Presl) Kubitzki, *Pandanus odorifer* (Forssk.) Kuntze, *Heliotropium arboreum* (Blanco) Mabb.

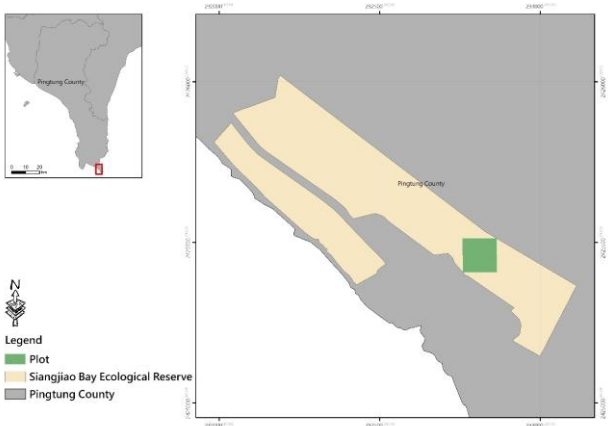

Figure 1. Distribution of study site in this study.

2.2 UAV Image Acquisition

A DJI Matrice 300 RTK unmanned aerial vehicle (UAV) equipped with a DJI Zenmuse P1 full-frame photogrammetric camera was used to acquire aerial imagery from June to August 2025. The P1 camera features a 45-megapixel full-frame CMOS sensor (pixel size: 4.4 μm) and a 35-mm prime lens, enabling high radiometric fidelity and fine-scale canopy structure detection suitable for vegetation monitoring and post-disturbance assessment.

Flight missions were planned using the DJI Pilot application in grid-based orthophoto mode. A terrain-following flight pattern was employed to maintain consistent ground sampling distance (GSD) across areas with elevation variability. All surveys were conducted at a nominal altitude of 150 m and a flight speed of 15 m/s, with 80% forward and 75% side overlap to ensure robust dense image matching and photogrammetric reconstruction. Each mission yielded approximately 700 images, covering 37.6 ha with a GSD of 1.88 cm/pixel.

The UAV’s onboard RTK module provided real-time kinematic positioning during each flight. To enhance absolute spatial accuracy, Post-Processed Kinematic (PPK) corrections were applied using reference data from the nearest Taiwan e-GNSS base station. In areas where satellite geometry or signal stability was limited, three temporary ground control points (GCPs) were installed and surveyed using an Emlid Reach RS2 GNSS receiver, achieving horizontal and vertical accuracies within 2–3 cm.

The DJI Zenmuse P1 camera is equipped with a standard RGB CMOS sensor without near-infrared (NIR) sensitivity. Therefore, the red, green, and blue channels are limited to the visible spectrum, and the NGRDI values derived in this study are based solely on visible reflectance without NIR contamination.

2.3 Calculation of Vegetation Indices

This study employed the Normalized Green–Red Difference Index (NGRDI), a visible-spectrum vegetation index based on differences between green and red reflectance (Tucker, 1979; Gitelson et al., 2002).

$$NGRDI = \frac{(Green - Red)}{(Green + Red)}$$

The NGRDI value theoretically ranges between –1 to +1. Positive values indicate dense vegetation with high chlorophyll content, values near zero correspond to sparse vegetation, and negative values represent bare surfaces or non-vegetated areas (Hunt et al., 2005; Meyer & Neto, 2008).

2.4 Canopy Gap Detection

NGRDI-derived vegetation coverage was combined with Digital Surface Model (DSM) data to analyze canopy height changes and identify potential gap areas. The DSMs were generated from UAV imagery using structure-from-motion (SfM) photogrammetry implemented in Pix4Dmapper.

By differencing DSMs from June and July 2025, regions exhibiting height reduction ($\Delta DSM < 0$) were identified and interpreted as potential canopy disturbance areas. These areas were spatially overlaid with corresponding NGRDI maps to analyze spectral responses associated with canopy loss.

The NGRDI threshold was determined based on the distribution of NGRDI values within DSM-derived canopy reduction areas. Observations indicated that NGRDI values in these regions predominantly ranged from –0.08 to 0.0325. Accordingly, an operational threshold of NGRDI < 0.03 was adopted to classify canopy gaps.

All image acquisitions were conducted under similar daylight conditions to minimize illumination variability. This consistency reduces the influence of temporal changes in solar angle and shadow patterns on NGRDI values. The overall workflow of this study is illustrated in Figure 2.

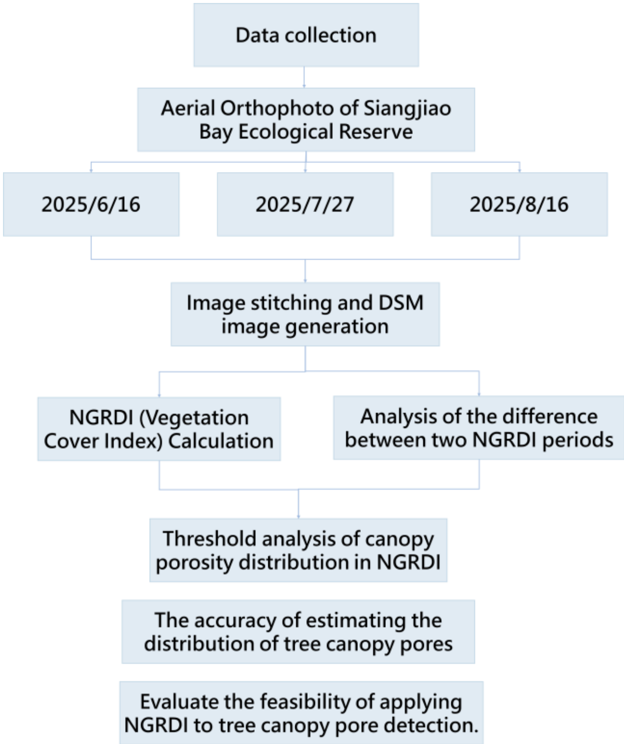

Figure 2. Research Process Planning

3. Results and Discussion

3.1 UAV Image Collection

This section provides a brief description of UAV data acquisition conditions to support the interpretation of temporal analysis results. Aerial surveys were conducted on 16 June (Figure 3), 27 July(Figure 4), and 16 August 2025 (Figure 5). The acquisition times for each survey were recorded to ensure consistency in illumination conditions across datasets. All image datasets were subsequently processed using Pix4Dmapper Pro to generate orthomosaics and digital surface models (DSMs), ensuring consistent radiometric and geometric correction across the three time periods.

Notably, the July acquisition was delayed due to the passage of Typhoon Danas, which affected Taiwan from 6 to 9 July 2025. The typhoon brought intense rainfall to southern Taiwan and, although it later weakened into a tropical depression, the strengthened southwest monsoon continued to deliver heavy precipitation in the subsequent days. These prolonged adverse weather conditions impeded UAV flight operations and resulted in a postponed image acquisition schedule. As a consequence, the July dataset reflects post-disturbance conditions that provide valuable insight into canopy responses following a major meteorological event.

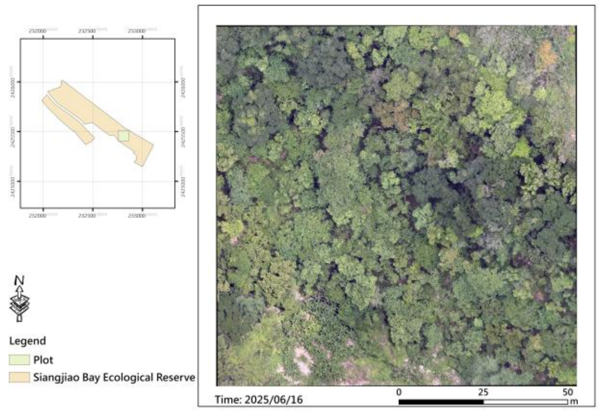

Figure 3. UAV-RGB imagery of the study site in June.

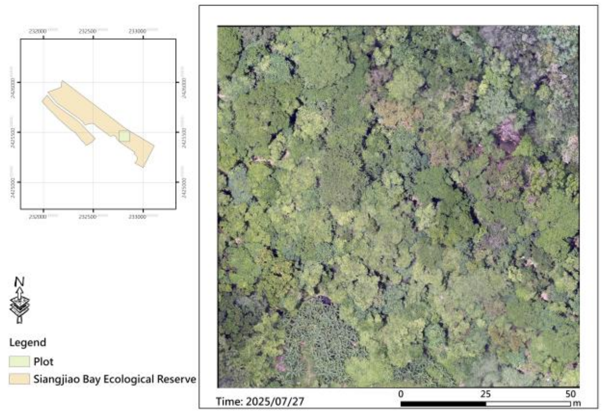

Figure 4. UAV-RGB imagery of the study site in July

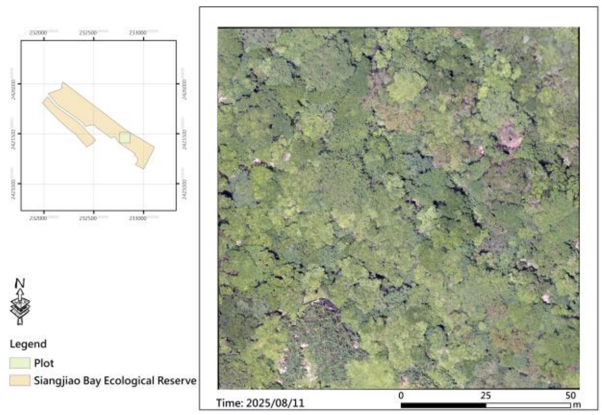

Figure 5. UAV-RGB imagery of the study site in August

Time-series analysis of UAV imagery collected over a three-month period reveals pronounced temporal variation in canopy structure within the study area. Imagery acquired immediately following Typhoon Danas exhibits clear evidence of mechanical disturbance, including crown fragmentation, branch breakage, and localized reductions in canopy cover. In contrast, imagery obtained approximately one month later (August) shows noticeable shifts in canopy-gap distribution, suggesting the onset of structural reorganization or partial recovery relative to the immediate post-disturbance condition. These short-term dynamics demonstrate that both canopy degradation and initial stages of recovery can manifest at detectable levels within a

https://doi.org/10.5194/isprs-archives-XLIX-B3-2026-325-2026

one-month timeframe, underscoring the rapid temporal sensitivity of forest canopies to severe wind disturbance.

These findings emphasize the responsiveness, temporal resolution, and operational flexibility of UAV-based monitoring for assessing fine-scale canopy dynamics. The observed patterns underscore the value of UAV imagery as a rapid assessment tool for evaluating forest structural conditions following extreme weather events, offering critical insights into both disturbance impacts and the initial phases of post-disturbance recovery.

Wind disturbances can induce immediate and substantial modifications to forest canopy architecture, including crown breakage, defoliation, and increased canopy openness (Boose et al., 1994; Kupfer et al., 2008). Structural damage caused by typhoons and hurricanes often triggers rapid reorganization of canopy gaps, with detectable changes emerging within weeks to several months as trees initiate re-foliation, branch regrowth, or exhibit early-stage mortality (Peereman et al., 2023; Xi et al., 2008). Such short-term structural adjustments have been widely documented in tropical and subtropical forests, where the initial phases of canopy recovery—or, in some cases, delayed decline—typically unfold within the first one to two months following severe wind events (Chen & Luyssaert, 2023), indicating the high temporal sensitivity of forest canopies to wind disturbances and underscoring the importance of fine-resolution monitoring for capturing early post-storm dynamics.

Furthermore, recent advances in UAV-based remote sensing have demonstrated its effectiveness for capturing fine-scale disturbance signatures and post-storm canopy reorganization. High-resolution UAV imagery enables precise quantification of canopy gaps, crown damage, and spatial heterogeneity that are often missed by satellite platforms (Dash et al., 2017; Mohan et al., 2017). Several studies highlight UAVs as a rapid, flexible, and cost-effective tool for post-cyclone and post-typhoon forest assessments, particularly where fast-changing canopy conditions require high temporal resolution monitoring (Furukawa et al., 2022). These findings corroborate the present study’s observation that canopy structural dynamics—both degradation and initial recovery—can be effectively captured within short timeframes following extreme weather events.

3.2 Accuracy Assessment of Canopy Gap Classification

Through the integration of NGRDI analysis from the July 2025 UAV imagery with the DSM difference between July and June, areas where canopy height decreased ($\Delta DSM < 0$) exhibited NGRDI values predominantly ranging from –0.08 to 0.0325 (Figure 6.). These zones correspond to locations where canopy structure was disrupted, resulting in reduced vegetation greenness and increased exposure of background surfaces. Based on this observed distribution, an operational threshold of NGRDI < 0.03 was established to identify canopy gap areas. The histogram of NGRDI values (not shown) further supports the selected threshold by illustrating the concentration of values within this range.

Comparisons with existing literature further support the validity of the identified threshold. Healthy vegetation typically exhibits higher NGRDI values (approximately 0.05–0.20), whereas bare soil, shaded areas, and other non-vegetated surfaces generally fall within lower or negative ranges (–0.10 to 0.05) (Gitelson et al., 2002; Viña et al., 2011). The –0.08 to 0.03 interval observed in this study closely aligns with these documented spectral characteristics associated with low-greenness or sparsely vegetated surfaces. Moreover, threshold ranges reported in earlier UAV-derived NGRDI studies (Zhang et al., 2019; Vianna et al., 2025) fall within a comparable spectral domain, providing additional support for the utility of this index in distinguishing intact canopy cover from structurally open conditions.

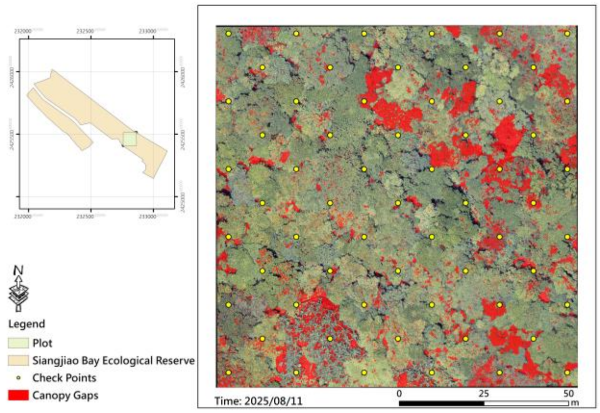

Figure 6. Tree canopy pore classification results and checkpoint distribution map

In the monitored area, canopy gaps covered a total of 1,634 m², accounting for 16.34% of the study plot. Accuracy assessment using 60 independent reference points yielded an overall classification accuracy of 93.33% and a Kappa coefficient of 0.68, indicating a substantial level of agreement. The model achieved 100% user accuracy and a commission error of 0% for the canopy-gap class, demonstrating a low rate of false detections. However, the omission error reached 44.44%, suggesting challenges in detecting small gaps or edge-derived openings that were identifiable during manual interpretation of the orthomosaic imagery.

The reference points were distributed systematically to ensure coverage across the study area. While this approach provides balanced spatial representation, it may not fully capture the irregular distribution of canopy gaps. Additionally, such sampling may introduce class imbalance when one class dominates, potentially influencing classification performance metrics. However, the current sampling design remains suitable for preliminary validation purposes. Future studies may consider stratified or object-based sampling approaches to better represent heterogeneous gap patterns and improve classification robustness. The classification accuracy is summarized in Table 1.

Table 1. Confusion Matrix and accuracy examining table for canopy gap classification.

Category		Image classification	
		Forest gap	Canopy
Manual Interpretation	Forest gap	5	4
	Canopy	0	51
User Accuracy(%)		100.00	
Producer Accuracy(%)		55.56	
Overall Accuracy(%)		93.33	
Commission Error(%)		0.00	
Omission Error(%)		44.44	
Kappa value		0.68	

The analysis indicated that an NGRDI threshold below 0.03 provided effective separation between canopy and non-canopy surfaces. Comparable threshold ranges have been reported elsewhere (Meyer & Neto, 2008; Vianna et al., 2024), suggesting broadly similar spectral behavior across vegetation conditions. Building on these relationships, the findings of Vianna et al. (2025) further demonstrated a positive association between NGRDI values and vegetation cover. Accordingly, within the context of forest or canopy monitoring, NGRDI values below 0.03 may serve as a practical preliminary indicator of areas with reduced canopy cover or potential non-canopy conditions, provided that additional structural or spatial information is used for verification.

The spectral behavior within this range can be attributed to several optical and structural mechanisms:

(1) Direct illumination of exposed background surfaces.
Canopy openings allow sunlight to reach the forest floor or lower vegetation layers, where soil, litter, or woody debris exhibit lower green reflectance, thereby reducing NGRDI values toward zero or negative ranges.

(2) Shadow-induced reflectance reduction.
Irregular shadow patterns created by canopy fragmentation simultaneously reduce green and red reflectance. Because both channels decrease proportionally, NGRDI values tend to cluster around zero, consistent with shadow-dominated pixels.

(3) Increased contribution of bare ground or litter reflectance.
Background materials typically have higher overall reflectance but lack the distinctive green reflectance of foliage, generating NGRDI values characteristic of non-vegetated surfaces.

(4) Vegetation thinning and mixed-pixel effects.
Post-disturbance canopy thinning increases the proportion of background reflectance within each pixel, lowering the NGRDI signal even in areas where some vegetation remains.

Taken together, these factors account for why canopy gaps or structurally damaged crowns consistently fall within the –0.08 to 0.03 NGRDI range. The close agreement between the empirical patterns observed in this study and the established spectral behavior of low-greenness surfaces supports the robustness of adopting NGRDI < 0.03 as an operational threshold for delineating canopy gaps. Nevertheless, variation in illumination conditions, species-specific reflectance properties, sensor exposure parameters, and seasonal shifts may influence index responses. Consequently, localized calibration is recommended when applying this threshold in different forest types, environmental settings, or time periods to ensure reliable and transferable gap-detection performance.

Although the threshold of NGRDI < 0.03 was found to be effective in this study, variations in threshold selection may influence classification outcomes. Future work should include sensitivity analysis using multiple threshold values derived from NGRDI histograms to further refine classification performance.

It is important to note that shadow effects may influence spectral responses in UAV imagery. Shadowed areas reduce reflectance in both red and green channels, often resulting in NGRDI values close to zero. However, such areas do not necessarily represent true canopy gaps. To address this limitation, DSM differencing was incorporated as a structural constraint. By integrating spectral (NGRDI) and structural (DSM) information, misclassification caused by shadow effects can be effectively reduced, improving the robustness of canopy gap detection.

In cases where DSM values do not indicate height reduction but NGRDI values fall below the threshold, such pixels are more likely associated with shadow effects or low-reflectance background rather than true canopy gaps. This observation also indicates the importance of combining spectral and structural information to ensure reliable classification.

The June and July datasets were primarily used for DSM differencing to detect structural changes, while the August dataset was used for spectral analysis and validation. This multi-temporal framework enables the integration of structural and spectral dynamics in canopy gap detection.

Although the analysis focused on the selected sample plot, similar spectral and structural patterns were consistently observed across the broader UAV coverage area, suggesting the method’s potential applicability for canopy gap detection at larger spatial scales.

4. Conclusion

In addition to NGRDI, other RGB-derived vegetation indices such as Excess Green Index (ExG) and Visible Atmospherically Resistant Index (VARI) may provide complementary information. Integrating multiple indices or applying machine learning approaches could further enhance classification accuracy and will be explored in future studies.

This study demonstrates the feasibility of applying the Normalized Green–Red Difference Index (NGRDI), derived from UAV-based RGB imagery, as an effective indicator for detecting forest canopy gaps. The results show that an operational threshold of NGRDI < 0.03 reliably differentiates canopy from non-canopy surfaces within the study area, achieving an overall classification accuracy of 93%. This threshold aligns with areas exhibiting structural disturbance or increased background exposure, highlighting the sensitivity of NGRDI to variations in canopy openness and confirming its utility for gap delineation in high-resolution UAV monitoring.

Although the model exhibited minimal commission errors, the presence of omission errors indicates that small or marginal canopy gaps remain difficult to detect when relying solely on NGRDI. Even so, the threshold-based approach provides a practical and efficient first-stage screening method for identifying potential gap regions. When complemented with structural datasets—such as DSM- or CHM-derived height differences—the accuracy of canopy-gap delineation can be substantially enhanced. These findings highlight the importance of integrating spectral and structural indicators to reduce misclassification and improve the detection of fine-scale or edge-derived canopy openings.

Importantly, the threshold identified in this study should not be regarded as universally applicable. NGRDI values are inherently influenced by illumination conditions, species-specific spectral characteristics, understory reflectance, and overall canopy density, indicating that contextual calibration remains essential for reliable interpretation. To enhance applicability across different forest types and temporal conditions, regional tuning and independent validation using height-based metrics—such as DSM or CHM differences—are recommended. These adjustments can help ensure consistent performance and improve the robustness of canopy-gap detection in diverse environmental settings.

Overall, the integration of UAV-derived RGB imagery with visible-spectrum vegetation indices provides a rapid and cost-effective framework for monitoring forest canopy conditions. The findings of this study indicate that an NGRDI threshold of < 0.03 can serve as an effective preliminary indicator for distinguishing canopy from non-canopy areas, particularly when supplemented by structural datasets for verification. This integrated approach offers substantial potential for operational monitoring, post-disturbance assessment, and long-term analyses of forest canopy dynamics, especially in contexts where LiDAR or multispectral sensing technologies are not readily accessible.

Acknowledgements

The successful completion of this study is made possible by the generous support and assistance of Associate Professor Chun-Hung Wei and Research Assistant Mr. Yong-Jun Zhang of the Department of Forestry at National Pingtung University of Science and Technology, Mr. Chi-Hua Chang of Heson Ecological Co., Ltd., and Mr. Mu-Yu Huang of Dicui Ecological Co., Ltd., as well as the help of other graduate students who participated in this project. Special thanks are extended to Professor Jan-Chang Chen, the principal investigator, for his guidance in research planning and implementation. We also wish to express their gratitude to members of the Remote Sensing Laboratory for their assistance with plot surveys, UAV image acquisition, and data processing. Furthermore, the contributions of the administrative and technical support teams in site inspections, equipment allocation, and project coordination are gratefully acknowledged. Their collective efforts made the successful completion of this study possible.

References

Biró, L., Kozma-Bognár, V., Berke, J., 2024. Comparison of RGB indices used for vegetation studies based on structured similarity index (SSIM). *Journal of Plant Science and Phytopathology*, https://doi.org/10.29328/journal.jpsp.1001124

Boose, E.R., Foster, D.R., Fluet, M., 1994. Hurricane impacts to tropical and temperate forest landscapes. *Ecological Monographs*, 64(4), 369–400.

Brokaw, N.V.L., 1982. The definition of treefall gap and its effect on measures of forest dynamics. *Biotropica*, 14(2), 158-160.

Chen, J., Li, W., Jucker, T., Da, H., 2023. Detecting forest canopy gaps using unoccupied aerial vehicle RGB imagery in a species-rich subtropical forest. *Remote Sensing in Ecology and Conservation*, 9(4). https://doi.org/10.1002/rse2.336

Chen, Y.-Y., Luyssaert, S., 2023. Tropical cyclones facilitate recovery of forest leaf area from dry spells in East Asia, *Biogeosciences*, 20, 349–363, https://doi.org/10.5194/bg-20-349-2023

Chung, C.-H., Wang, J., Deng, S.-L., Huang, C.-Y., 2022. Analysis of Canopy Gaps of Coastal Broadleaf Forest Plantations in Northeast Taiwan Using UAV Lidar and the Weibull Distribution. *Remote Sens*, 14, 667. https://doi.org/10.3390/rs14030667

Dash, J.P., Watt, M.S., Pearse, G.D., Heaphy, M., Dungey, H.S., 2017. Assessing very high resolution UAV imagery for monitoring forest health during a simulated disease outbreak. ISPRS Journal of Photogrammetry and Remote Sensing, 131, https://doi.org/10.1016/j.isprsjprs.2017.07.007

Furukawa, F., Morimoto, J., Yoshimura, N., Koi, T., Shibata, H., Kaneko, M., 2022. UAV Video-Based Approach to Identify Damaged Trees in Windthrow Areas. Remote Sens, 14, 3170. https://doi.org/10.3390/rs14133170

Gaulton, R., Malthus, T., 2008. LiDAR mapping of canopy gaps in continuous cover forests: A comparison of canopy height model and point cloud based techniques. *International Journal of Remote Sensing*, 31(5):17-19.

Gitelson, A.A., Kaufman, Y.J., Stark, R., Rundquist, D., 2002. Novel algorithms for remote estimation of vegetation fraction. *Remote Sensing of Environment*, 80(1), 76–87.

Htun, N.M., Owari, T., Tsuyuki, S., Hiroshima, T., 2024. Detecting Canopy Gaps in Uneven-Aged Mixed Forests through the Combined Use of Unmanned Aerial Vehicle Imagery and Deep Learning. *Drones*, 8, 484. https://doi.org/10.3390/drones8090484

Hunt, E.R., Cavigelli, M., Daughtry, C.S. T., McMurtrey, J.E., Walthall, C.L., 2005. Evaluation of digital photography from model aircraft for remote sensing of crop biomass and nitrogen status. *Precision Agriculture*, 6(4), 359–378.

Krüger, K., Senf, C., Jucker, T., Pflugmacher, D., 2024. Gap expansion is the dominant driver of canopy openings in a temperate mountain forest landscape. *Journal of Ecology*, https://doi.org/10.1111/1365-2745.14320

Kupfer, J.A., Myers, A.T., McLane, S.E., Melton, G.N., 2008. Patterns of forest damage in a southern Mississippi landscape caused by Hurricane Katrina. *Ecosystems,* 11, 45–60.

Lenk, A., Richter, R., Kretz, L., Wirth, C., 2024. Effects of canopy gaps on microclimate, soil biological activity and their relationship in a European mixed floodplain forest. *Science of The Total Environment*, 941. https://doi.org/10.1016/j.scitotenv.2024.173572

Mazdi, R.A., Mataji, A., Fallah, A., 2021. Canopy gap dynamics, disturbances, and natural regeneration patterns in a beech-dominated Hyrcanian old-growth forest. *Baltic Forestry*, 27(1): 535. https://doi.org/10.46490/BF535.

Meyer, G.E., Neto, J.C., 2008. Verification of color vegetation indices for automated crop imaging applications. *Computers and Electronics in Agriculture,* 63(2), 282–293.

Mohan, M., Silva, C.A., Klauberg, C., Jat, P., Catts, G., Cardil, A., Hudak, A.T., Dia, M., 2017. Individual tree detection from Unmanned Aerial Vehicle (UAV) derived canopy height model in an open canopy mixed *Conifer* forest. *Forests*, *8*(9), 340, https://doi.org/10.3390/f8090340

Muscolo, A., Bagnato, S., Sidari, M., Mercurio, R., 2014. A review of the roles of forest canopy gaps. *Journal of Forestry Research*, 25(4), 725–736.

Peereman, J., Hogan, J.A., Lin, T.C., 2023. Intraseasonal interactive effects of successive typhoons characterize canopy damage of forests in Taiwan: A remote sensing-based assessment. Forest Ecology and Management, 521, https://doi.org/10.1016/j.foreco.2022.120430

Simonetti, A., Araujo, R.F., Celes, C.H.S., da Silva e Silva, F.R., dos Santos, J., Higuchi, N., Trumbore, S., Magnabosco Marra, D., 2023. Canopy gaps and associated losses of biomass – combining UAV imagery and field data in a central Amazon forest. *Biogeosciences*, 20, 3651–3666, https://doi.org/10.5194/bg-20-3651-2023

Tian, A., Halik, Ü., Fu, W.; Sawirdin, S., Cheng, S., Lei, J., 2024. Research History of Forest Gap as Small-Scale Disturbances in Forest Ecosystems. *Forests*, 15, 21. https://doi.org/10.3390/f15010021

Tucker, C.J., 1979. Red and photographic infrared linear combinations for monitoring vegetation. *Remote Sensing of Environment*, 8(2), 127–150.

Vianna, M.S., Matias, F.I., Galli, G., Martins, E.S., Oliveira, M., Pinheiro, J.B., 2025. Using red–green–blue vegetation indices to evaluate complex agronomical traits in soybean breeding. *Agronomy Journal*, 117(1), e21723, https://doi.org/10.1002/agj2.21723

Viña, A., Gitelson, A.A., Nguy-Robertson, A.L., Peng, Y., 2011. Comparison of different vegetation indices for the remote assessment of green leaf area index of crops. *Remote Sensing of Environment*, 115(12): 3468-3478. https://doi.org/10.1016/j.rse.2011.08.010

Whitmore, T.C., 1989. Canopy gaps and the two major groups of forest trees. *Ecology*, 70(3), 536–538.

Winstanley, P., Dalagnol, R., Mendiratta, S., Braga, D., Galvão, L.S., Bispo, P.d.C., 2024. Post-Logging canopy gap dynamics and forest regeneration assessed using airborne LiDAR time series in the Brazilian Amazon with attribution to gap types and origins. *Remote Sens*, 16, 2319. https://doi.org/10.3390/rs16132319

Xi, W., Peet, R.K., Urban, D.L., 2008. Changes in forest structure, species diversity and spatial pattern following hurricane disturbance in a Piedmont North Carolina forest, USA, *Journal of Plant Ecology*, 1(1): 43–57, https://doi.org/10.1093/jpe/rtm003

Zhang, D., Liu, J., Ni, W., Sun, G., Zhang, Z., Liu, Q., Wang, Q., 2019. Estimation of forest leaf area index using height and canopy cover information extracted from unmanned aerial vehicle stereo imagery. IEEE Journal of Selected Topics in Applied Earth Observations and Remote Sensing, 99: 1-11. https://doi.org/10.1109/JSTARS.2019.2891519

Zhu, J., Lu, D., Zhang, W., 2014. Effects of gaps on regeneration of woody plants: a meta-analysis. *Journal of Forestry Research*, 25: 501-510.